

# Generalized ABCD propagation for interacting atomic clouds.

F. Impens<sup>1,2</sup> and Ch. J. Bordé<sup>1,3</sup>

<sup>1</sup> *SYRTE, Observatoire de Paris, CNRS, 61 avenue de l'Observatoire, 75014 Paris, France*

<sup>2</sup> *Instituto de Física, Universidade Federal do Rio de Janeiro. Caixa Postal 68528, 21941-972 Rio de Janeiro, RJ, Brasil and*

<sup>3</sup> *Laboratoire de Physique des Lasers, Institut Galilée, F-93430 Villetaneuse, France*

(Dated: November 16, 2018)

We present a treatment of the nonlinear matter wave propagation inspired from optical methods, which includes interaction effects within the atom optics equivalent of the aberrationless approximation. The atom-optical ABCD matrix formalism, considered so far for non-interacting clouds, is extended perturbatively beyond the linear regime of propagation. This approach, applied to discuss the stability of a matter-wave resonator involving a free-falling sample, agrees very well with the predictions of the full nonlinear paraxial wave equation. An alternative optical treatment of interaction effects, based on the aberrationless approximation and suitable for cylindrical paraxial beams of uniform linear density, is also adapted for matter waves.

PACS numbers: 03.75.Pp, 03.75.-b, 42.65.Jx, 41.85.Ew, 31.15-Md

## I. INTRODUCTION

Light and matter fields are governed by similar equations of motion [1]. Both photons and atoms interact in a symmetrical manner: atom-atom interactions are mediated through photons, while photon-photon interactions are mediated through atoms. Before the advent of Bose-Einstein condensation, two groups realized independently that atomic interactions give rise to a cubic nonlinearity in the propagation equation analogous to that induced by the Kerr effect [2, 3]. Following this analogy, the field of non-linear atom optics emerged in the last decade, leading to the experimental verification with matter waves of several well-known nonlinear optical phenomena[i]: the four-wave mixing [9], the formation of solitons [10, 11, 12, 13] and of vortices [14, 15], the superradiance [16] and the coherent amplification [17]. The nonlinear propagation of matter waves has been the object of extensive experimental [18, 19] and theoretical work, among which the time-dependent Thomas-Fermi approximation [20], the variational approach [21], and the method of moments [22]. These treatments have been used successfully to obtain analytical expressions in good agreement with the exact solution of the 3D nonlinear Schrödinger equation (NLSE).

There exists, for cylindrical wave-packets propagating in the paraxial regime, a very elegant method to handle this equation which has been used in optics to treat self-focusing effects [23, 24]. It relies on the “aberrationless approximation”, assuming that the nonlinearity is sufficiently weak as to preserve the shape of a fundamental Gaussian mode, and it involves a

generalized complex radius of curvature. This treatment is equally relevant for the paraxial propagation of cylindrical matter waves, and it is presented in this context in Appendix A. Unfortunately, the assumptions required - such as the constant longitudinal velocity and the paraxial propagation - limit the scope of this approach, which appears as too stringent to describe the matter wave propagation in most experiments.

This motivates the introduction of a different analytical method to obtain approximate solutions for the NLSE in a more general propagation regime. This is the central contribution of this paper, which exposes a perturbative matrix analysis especially well-suited to discuss the stability of a matter-wave resonator. With an Hamiltonian quadratic in position and momentum operators, and in the absence of atomic interactions, the Schrödinger equation admits a basis of Gaussian solutions. Their evolution is easily obtained through a time-dependent matrix denoted “ABCD” [1, 25], in analogy with the propagation of optical rays in optics [26]. In the “aberrationless approximation”, it is possible to extend this treatment to include perturbatively interaction effects and obtain the propagation of a fundamental Gaussian mode with a modified “ABCD” matrix. As an illustration of this method, the stability of a matter-wave resonator is analyzed thanks to this “ABCD” matrix, which encapsulates the divergence resulting from the mean-field potential. An ABCD-matrix approach had already been used in [18] to characterize the divergence of a weakly outcoupled atom laser beam due to interactions with the source condensate. The present treatment is sensibly different, since it is not restricted to the paraxial regime and since it addresses rather self-interaction effects in the beam propagation. An “ABCD” matrix, including self-focusing effects, is computed in Sec. IV, and used to model the propagation of an atomic sample in a matter-wave resonator. Self-focusing is also discussed through an alternative method exposed in Appendix A.

[i] Many other optical phenomena have also been verified with matter waves. A short list includes interferences [4] and diffraction phenomena [3, 5], the temporal Talbot effect [6], and the influence of spatial phase fluctuations on interferometry [7]. New effects arise also with rotating condensates [8].

Our approach is indeed mainly inspired from previous theoretical developments in optics, which aimed at treating the wave propagation in a Kerr medium through such a matrix formalism [23]. An approach of the non-linearity based on the resulting frequency-dependent diffraction [27] successfully explained the asymmetric profile of atomic and molecular intra-cavity resonances [28], as well as the dynamics of Gaussian modes in ring and two-isotopes lasers [29, 30]. Later, a second-order polynomial determined by a least-square fit of the wave intensity profile was considered to model the Kerr effect [31]. In this paper, we explore the quantum mechanical counterpart of this strategy: mean-field interactions are modelled thanks to a second-order polynomial, determined perturbatively from the wave-function, and which can be interpreted in optical terms.

## II. LENSING POTENTIAL

One considers the propagation of a zero-temperature condensate in a uniform gravity field and in the mean-field approximation. The corresponding Hamiltonian reads:

$$\hat{H} = \frac{\hat{\mathbf{p}}^2}{2m} + mgz + g_I |\phi(\hat{\mathbf{r}}, t)|^2 \quad (1)$$

$g_I$  is the coupling constant related to the s-wave scattering length  $a$  and to the number of atoms  $N$  by  $g_I = 4\pi N \hbar^2 a / m$ . Our purpose is to approximate the mean-field potential  $g_I |\phi(\mathbf{r}, t)|^2$  by an operator leading to an easily solvable wave equation and as close as possible to the interaction potential. A second-order polynomial in the position and momentum operators is a suitable choice, since it allows to obtain Gaussian solutions to the propagation equation. These solutions are approximate, but they lead nonetheless to a satisfactory description of the propagation of diluted atomic wave-packets and of their stability in resonators, which are the issues addressed in this paper. We note  $\hat{H}_0 = \frac{\hat{\mathbf{p}}^2}{2m} + mgz$  the interaction-free Hamiltonian and

$$\hat{H}(\hat{\mathbf{r}}, \hat{\mathbf{p}}, t) = \hat{H}_0 + P_l(\hat{\mathbf{r}}, \hat{\mathbf{p}}, t) \quad (2)$$

the quadratic Hamiltonian accounting for interactions effects.

The strategy exposed in this paper consists in picking up, among the possible polynomials  $P$ , the element which minimizes an appropriate distance measure to the mean-field potential. In geometric terms, this polynomial appears as the projection of the mean-field potential onto the vector space spanned by second-order polynomials in position and momentum. This potential will be referred to as the ‘‘lensing potential’’, denomination which will be justified in Sec. IV. We define a distance analogous to the error function used in [31], which involves the polynomial  $P$  and the quantum state  $|\phi(t)\rangle$  resulting from the

non-linear evolution:

$$E(P(t), |\phi(t)\rangle) = \int d^3\mathbf{r} |\langle \mathbf{r} | P(\hat{\mathbf{r}}, \hat{\mathbf{p}}, t) |\phi(t)\rangle - g_I |\phi(\mathbf{r}, t)|^2 \phi(\mathbf{r}, t) \rangle|^2 \quad (3)$$

The minimization of the distance  $E(P(t), |\phi(t)\rangle)$  for the lensing potential  $P_l(t)$  implies that the function  $E$  is stationary towards any second-order polynomial coefficient at the point  $(P_l(t), |\phi(t)\rangle)$ :

$$\forall t \geq t_0 \quad \nabla_P E(P_l(t), |\phi(t)\rangle) = 0 \quad (4)$$

We have noted  $\nabla_P$  the gradient associated with the coefficients of a second-order polynomial, and  $t_0$  is the initial time from which we compute the evolution of the wave-function - we assume that  $\phi(\mathbf{r}, t_0)$  is known -. The determination of the lensing potential associated with self-interactions in the beam indeed requires previous knowledge of the wave-function evolution. This difficulty did not arise in other optical treatments of atomic interaction effects [18, 32, 33], in which the atomic beam propagation was mainly affected by interactions with a different sample of well-known wave-function. This is typically the case for a weakly outcoupled continuous atom laser beam, in which the diverging lens effect results from the source condensate. We propose to circumvent this self-determination problem thanks to a perturbative treatment. Such approach is legitimate for the diluted matter waves involved in usual atom interferometers. The first-order lensing polynomial and the corresponding Hamiltonian  $\hat{H}^{(1)}(t) = \hat{H}_0 + P_l^{(1)}(\hat{\mathbf{r}}, \hat{\mathbf{p}}, t)$  are determined from the linear evolution, according to:

$$\forall t \geq t_0 \quad \nabla_P E\left(P_l^{(1)}(t), e^{-i/\hbar \hat{H}_0(t-t_0)} |\phi(t_0)\rangle\right) = 0 \quad (5)$$

Higher-order lensing effects can be computed iteratively. For instance, the second-order lensing polynomial  $P_l^{(2)}(t)$  satisfies at any instant  $t \geq t_0$ :

$$\nabla_P E\left(P_l^{(2)}(t), T\left[e^{-i/\hbar \int_{t_0}^t dt' [\hat{H}_0 + P_l^{(1)}(\hat{\mathbf{r}}, \hat{\mathbf{p}}, t')]} |\phi(t_0)\rangle\right]\right) = 0$$

where we have used the usual time-ordering operator  $T$  [34].

## III. OPTICAL PROPAGATION OF MATTER WAVES: THE ABCD THEOREM.

This section gives a remainder on a general result - called the ABCD theorem - concerning the propagation of matter waves in a time-dependent quadratic potential, which is the atomic counterpart of the ray matrix formalism frequently used in optics [26]. It shows that the evolution of a Gaussian wave-function under an Hamiltonian quadratic in position and momentum is similar to the propagation of a Gaussian mode of the electric field in a linear optical system. A detailed description of this theoretical result of atom optics is

given in the references [25, 35].

One considers a time-dependent quadratic Hamiltonian such as:

$$\hat{H}_0 + P(\hat{\mathbf{r}}, \hat{\mathbf{p}}, t) = \frac{\hat{\mathbf{p}}\hat{\beta}(t)\hat{\mathbf{p}}}{2m} + \frac{1}{2}\hat{\mathbf{p}}\alpha(t)\hat{\mathbf{r}} - \frac{1}{2}\hat{\mathbf{r}}\delta(t)\hat{\mathbf{p}} - \frac{m}{2}\hat{\mathbf{r}}\gamma(t)\hat{\mathbf{r}} - m\mathbf{g}(t) \cdot \hat{\mathbf{r}} + \mathbf{f}(t) \cdot \hat{\mathbf{p}} + h(t) \quad (6)$$

$\alpha(t)$ ,  $\beta(t)$ ,  $\gamma(t)$  and  $\delta(t)$  are  $3 \times 3$  matrices [ii];  $\mathbf{f}(t)$  and  $\mathbf{g}(t)$  are three-dimensional vectors;  $h(t)$  is a scalar, and  $\sim$  stands for the transposition. Here we use this Hamiltonian to approximate the nonlinear Hamiltonian (1). The Hamiltonian (6) is indeed appropriate to describe several physical effects [36, 37].

### A. ABCD propagation of a Gaussian wave-function.

The propagation of a Gaussian wave-packet in such an Hamiltonian can be described simply as follows. Let  $\phi(\mathbf{r}, t)$  be an atomic wave packet initially given by:

$$\phi(\mathbf{r}, t_0) = \frac{1}{\sqrt{|\det X_0|}} e^{\frac{im}{2\hbar}(\mathbf{r}-\mathbf{r}_{c0})Y_0X_0^{-1}(\mathbf{r}-\mathbf{r}_{c0}) + \frac{i}{\hbar}\mathbf{p}_{c0} \cdot (\mathbf{r}-\mathbf{r}_{c0})} \quad (7)$$

The  $3 \times 3$  complex matrices  $X_0$ ,  $Y_0$  represent the initial width of the wave packet in position and momentum respectively:  $X_0 = iD(\Delta x(t_0), \Delta y(t_0), \Delta z(t_0))$  and  $Y_0 = D(\Delta p_x(t_0), \Delta p_y(t_0), \Delta p_z(t_0))$ , with  $D$  standing for a diagonal matrix. The vectors  $\mathbf{r}_{c0}$ ,  $\mathbf{p}_{c0}$  give the initial average position and momentum. The ABCD theorem for matter waves states that, at any time  $t \geq t_0$ , the wave-packet  $\phi(\mathbf{r}, t)$  satisfies:

$$\phi(\mathbf{r}, t) = \frac{e^{\frac{i}{\hbar}S(t, t_0, \mathbf{r}_{c0}, \mathbf{p}_{c0})}}{\sqrt{|\det X_t|}} e^{\frac{im}{2\hbar}(\mathbf{r}-\mathbf{r}_{ct})Y_tX_t^{-1}(\mathbf{r}-\mathbf{r}_{ct}) + \frac{i}{\hbar}\mathbf{p}_{ct} \cdot (\mathbf{r}-\mathbf{r}_{ct})}$$

$S(t, t_0, \mathbf{r}_{c0}, \mathbf{p}_{c0})$  is the classical action evaluated between  $t$  and  $t_0$  of a point-like particle which motion follows the classical Hamiltonian  $H(\mathbf{r}, \mathbf{p}, t)$  and with respective initial position and momentum  $\mathbf{r}_{c0}$ ,  $\mathbf{p}_{c0}$ . The width matrices in position  $X_t$  and momentum  $Y_t$ , and the average position and momentum  $\mathbf{r}_{ct}$ ,  $\mathbf{p}_{ct}$  at time  $t$  are determined through the same  $6 \times 6$  ‘‘ABCD’’ matrix:

$$\begin{pmatrix} \mathbf{r}_{ct} \\ \frac{1}{m}\mathbf{p}_{ct} \end{pmatrix} = \begin{pmatrix} A(t, t_0) & B(t, t_0) \\ C(t, t_0) & D(t, t_0) \end{pmatrix} \begin{pmatrix} \mathbf{r}_{c0} \\ \frac{1}{m}\mathbf{p}_{c0} \end{pmatrix} + \begin{pmatrix} \xi(t, t_0) \\ \phi(t, t_0) \end{pmatrix}$$

$$\begin{pmatrix} X_t \\ Y_t \end{pmatrix} = \begin{pmatrix} A(t, t_0) & B(t, t_0) \\ C(t, t_0) & D(t, t_0) \end{pmatrix} \begin{pmatrix} X_0 \\ Y_0 \end{pmatrix}$$

The ABCD matrix -noted compactly  $M(t, t_0)$ - and the vectors  $\xi$ ,  $\phi$  can be expressed formally as [37]:

$$M(t, t_0) = T \left[ \exp \left( \int_{t_0}^t dt' \begin{pmatrix} \alpha(t') & \beta(t') \\ \gamma(t') & \delta(t') \end{pmatrix} \right) \right] \quad (8)$$

$$\begin{pmatrix} \xi(t, t_0) \\ \phi(t, t_0) \end{pmatrix} = \int_{t_0}^t dt' M(t, t') \begin{pmatrix} \mathbf{f}(t') \\ \mathbf{g}(t') \end{pmatrix} \quad (9)$$

Although the former expressions seem rather involved, in all cases of practical interest, the  $ABCD\xi\phi$  parameters can be determined analytically or at least by efficient numerical methods.

### B. Interpretation of the ABCD propagation and aberrationless approximation.

The phase-space propagation provides a relevant insight in the transformation operated by the ABCD matrix. Consider the Wigner distribution of a single-particle density operator evolving under the Hamiltonian (6). The Wigner distribution at time  $t$  is related to the distribution at time  $t_0$  by the following map:

$$W(\mathbf{r}, \mathbf{p}, t) = W \left( \tilde{D}(\mathbf{r} - \xi) - \frac{1}{m}\tilde{B}(\mathbf{p} - m\phi), -m\tilde{C}(\mathbf{r} - \xi) + \tilde{A}(\mathbf{p} - m\phi), t_0 \right)$$

where the matrices  $A, B, C, D$  and vectors  $\xi, \phi$  are again evaluated at the couple of instants  $(t, t_0)$ . The action of the evolution operator onto the Wigner distribution is thus amenable to a time-dependent linear map. The fact that ABCD matrices are symplectic [25] implies that this map is unitary: such evolution preserves the global phase-space volume, and the quality factor of an atomic beam in the sense of [38].

In photon as in atom optics, the aberrationless approximation consists in assuming that the Gaussian function (7) is a self-similar solution of the propagation equation in spite of the non-linearity, the evolution of which is given by the ABCD propagation. The propagation is thus described through a map which preserves the phase-space density. This is an approximation, since for atomic or light beams evolving in nonlinear media, the phase-space density indeed changes during the propagation. Nonetheless, the aberration-less approximation is reasonable for sufficiently diluted clouds, subject to a weak mean-field interaction term, for which an initially Gaussian wave-function will not couple significantly to higher-order modes. Furthermore, this approximation in atom optics is entirely analogous to the aberration-free treatment realized in non-linear optics, the predictions of which concerning the width evolution of a light beam have been verified experimentally [39]. One can thus expect that the aberrationless approximation will constitute a good description of the propagation in atom optics as well. Indeed, the validity of the aberrationless approximation will be confirmed in Sec. V D on the example of

[ii]  $\delta(t) = -\tilde{\alpha}(t)$  to ensure the Hamiltonian hermiticity

a gravitational atomic resonator: its predictions on the sample size evolution are in good agreement with those of a paraxial treatment of the wave-function propagation which does not assume the preservation of a Gaussian shape.

#### IV. ABCD MATRIX OF A FREE-FALLING INTERACTING ATOMIC CLOUD.

Let us apply the method discussed above to describe the propagation of a free-falling Gaussian atomic wave-packet. In the aberrationless approximation, such a wave-packet is simply determined by the parameters  $ABCD\xi\phi$  and by the phase associated with the action. In view of the resonator stability analysis, we will focus on the computation of the ABCD matrix in presence of the mean-field potential. We consider only the leading-order nonlinear corrections, associated with the first-order lensing polynomial  $P_l^{(1)}(\mathbf{r}, \mathbf{p}, t)$ .

This section begins with the determination of this potential defined by Eq.(5). A formal expression of the atom-optical ABCD matrix, taking into account this lensing potential, is obtained. An infinitesimal expansion of this expression shows that the mean-field interactions effectively play the role of a divergent lens: the atom-optical ABCD matrix of the free-falling cloud evolution is similar to the optical ABCD matrix associated with the propagation of a light ray through a series of infinitesimal divergent lenses. In our case, the propagation axis is the time, and the infinitesimal lenses correspond to the action of the mean-field potential in infinitesimal time slices.

##### A. Determination of the lensing potential.

We assume that the condensate, evolving in the Hamiltonian (1), is initially at rest and described by a Gaussian wave-function:

$$\phi(x, y, z, t_0) = \frac{\pi^{-3/4}}{\sqrt{w_{x0}w_{y0}w_{z0}}} e^{-\frac{x^2}{2w_{x0}^2} - \frac{y^2}{2w_{y0}^2} - \frac{z^2}{2w_{z0}^2}} \quad (10)$$

It is easy to show that, when one considers the interaction-free evolution, the widths are given at time  $t \geq t_0$  by:

$$w_{it} = \sqrt{w_{i0}^2 + \frac{\hbar^2}{m^2 w_{i0}^2} (t - t_0)^2} \quad (11)$$

for  $i = x, y, z$ . This result can be easily retrieved by considering the initial width matrices  $X_0 = iD(w_{x0}, w_{y0}, w_{z0})$  and  $Y_0 = \frac{\hbar}{m}D(1/w_{x0}, 1/w_{y0}, 1/w_{z0})$  for the wave-function, and applying the free ABCD matrix [25]:

$$\begin{pmatrix} A(t, t_0) & B(t, t_0) \\ C(t, t_0) & D(t, t_0) \end{pmatrix} = \begin{pmatrix} 1 & t - t_0 \\ 0 & 1 \end{pmatrix}$$

The square of the free-evolving wave-function thus reads:

$$|\phi^{(0)}(\mathbf{r}, t)|^2 = \frac{\pi^{-3/2}}{w_{xt}w_{yt}w_{zt}} e^{-\frac{(x-x_{ct})^2}{w_{xt}^2} - \frac{(y-y_{ct})^2}{w_{yt}^2} - \frac{(z-z_{ct})^2}{w_{zt}^2}}$$

We use this expression to determine the first-order lensing polynomial  $P_l^{(1)}(\mathbf{r}, \mathbf{p}, t)$ . Since this operator acts on Gaussian wave-functions, differentiation is equivalent to the multiplication by a position coordinate, so the action of the momentum operator is indeed equivalent to that of the position operator up to a multiplicative constant. One can thus, without any loss of generality, search for a lensing polynomial  $P_l^{(1)}(\mathbf{r}, t)$  involving only the position operator. With this choice, the error function (3) minimized by the polynomial  $P$  becomes simply:

$$E(P(t), |\phi^{(0)}(t)\rangle) = \int d^3\mathbf{r} |\phi^{(0)}(\mathbf{r}, t)|^2 \left( P(\mathbf{r}, t) - g_I |\phi^{(0)}(\mathbf{r}, t)|^2 \right)^2$$

Expanding the polynomial  $P_l^{(1)}(\mathbf{r}, t)$  around the central position  $\mathbf{r}_{ct}$ , a parity argument shows that the linear terms vanish:

$$P_l^{(1)}(\mathbf{r}, t) = g_I [c_0(t) - c_x(t)(x - x_{ct})^2 - c_y(t)(y - y_{ct})^2 - c_z(t)(z - z_{ct})^2]$$

By definition of the lensing polynomial, the error function (12) must be stationary with respect to each coefficient  $c_{x,y,z,0}(t)$ , which leads to:

$$c_0(t) = \frac{7}{4V(t)}, \quad c_{x,y,z}(t) = \frac{1}{2w_{x,y,z}^2 V(t)},$$

with  $V(t) = (2\pi)^{3/2} w_{xt} w_{yt} w_{zt}$  (12)

Only the quadratic term intervene in the ABCD matrix: the coefficient  $c_0(t)$  merely adds a global additional phase to the wave-function, which does not change the subsequent stability analysis.

##### B. Formal expression of the effective ABCD matrix.

We can readily express the ABCD matrix associated with the evolution under  $\hat{H}^{(1)}(t)$ . Writing this Hamiltonian in the form of Eq. (6), and using the formal expression (8) of the ABCD matrix as a time-ordered series, one obtains:

$$M^{(1)}(t, t_0, X_0) = T \left[ \exp \left( \int_{t_0}^t dt' \begin{pmatrix} \alpha(t') & \beta(t') \\ \gamma(t') & \delta(t') \end{pmatrix} \right) \right] \quad (13)$$

In contrast to the usual linear ABCD matrices, this matrix now depends on the input vector through the initial position width matrix  $X_0$  [iii]. A brief inspection of Eq.

[iii] The Hamiltonian  $\hat{H}^{(1)}(t)$  and the lensing polynomial  $P_l^{(1)}(\mathbf{r}, t)$  depend of course also on  $X_0$ , but we do not mention this dependence explicitly to alleviate the notations.

(6) and of the Hamiltonian  $\hat{H}^{(1)}(t)$

$$\hat{H}^{(1)}(t) = \frac{\hat{\mathbf{p}}^2}{2m} + mg\hat{z} + g_I [c_0(t) - c_x(t)(\hat{x} - x_{ct})^2 - c_y(t)(\hat{y} - y_{ct})^2 - c_z(t)(\hat{z} - z_{ct})^2], \quad (14)$$

shows that the matrices in the exponential read  $\alpha(t) = \delta(t) = 0$ ,  $\beta(t) = 1$  and  $\gamma(t) = \frac{2g_I}{m} \mathbf{D}(c_x(t), c_y(t), c_z(t))$ . Using Eq. (12), one readily obtains the elements of the quadratic matrix  $\gamma$ :

$$\gamma_{ii}(t) = \frac{g_I}{m} \frac{1}{w_{it}^2(w_{xt}w_{yt}w_{zt})} \quad (15)$$

for  $i = x, y, z$ , with the widths  $w_{x,y,z,t}$  given by Eq. (11). A significant simplification arises because  $\gamma(t)$  is diagonal: one needs only to compute the exponential of three  $2 \times 2$  matrices associated with the orthogonal directions  $O_x, O_y, O_z$ . The ABCD matrix is simply the tensor product of those:

$$M^{(1)}(t, t_0, X_0) = \otimes_{i=x,y,z} T \left[ \exp \left( \int_{t_0}^t dt' \begin{pmatrix} 0 & 1 \\ \gamma_{ii}(t') & 0 \end{pmatrix} \right) \right] \quad (16)$$

### C. Propagation in a series of infinitesimal lenses.

An infinitesimal expansion of (18) shows that the evolution between  $t$  and  $t + dt$  is described by the ABCD matrix:

$$M^{(1)}(t + dt, t, X_0) \simeq \begin{pmatrix} 1 & dt \\ \gamma(t) & 1 \end{pmatrix} \quad (17)$$

It can be rewritten as a product of two ABCD matrices:

$$M^{(1)}(t + dt, t, X) \simeq \begin{pmatrix} 1 & dt \\ 0 & 1 \end{pmatrix} \begin{pmatrix} 1 & 0 \\ \gamma(t) & 1 \end{pmatrix} \quad (18)$$

If these were  $2 \times 2$  matrices, in the optical formalism, the first matrix would be associated with the propagation of a ray on the length  $dt$  and the second matrix, of the form

$$\begin{pmatrix} 1 & 0 \\ -dt/f & 1 \end{pmatrix} \quad (19)$$

would model a lens of infinitesimal curvature  $dt/f$ . One can thus consider, by analogy, that this second  $6 \times 6$  matrix realizes an atom-optical lens which curvature is the infinitesimal  $3 \times 3$  matrix  $\mathbf{D}(\gamma_{xx}(t), \gamma_{yy}(t), \gamma_{zz}(t)) dt$ . Besides, one can exploit the fact that it is a tensor product: if one considers each direction  $O_x, O_y, O_z$  separately, the propagation amounts - as in optics - to a product of  $2 \times 2$  matrices, which makes the analogy with a lens even more transparent. The resulting  $6 \times 6$  ABCD matrix is simply given by the tensor product of those. Transverse degrees of freedom are, nonetheless, coupled to each other through the lensing potential. It is worth noticing that the focal lengths  $f_x, f_y, f_z$  have here the dimension of a time, and are negative if one considers repulsive interactions: the quadratic potential  $P_l^{(1)}(\mathbf{r}, \mathbf{p}, t)$  acts as a series of diverging lenses associated with each infinitesimal time slice.

### D. Expression of the nonlinear ABCD matrix with the Magnus Expansion.

Because of the time-dependence of the Hamiltonian  $\hat{H}^{(1)}(t)$ , the time-ordered exponential in (18) cannot, in general, be expressed analytically. Fortunately, a useful expression is provided by the Magnus expansion [40]:

$$M^{(1)}(t, t_0, X_0) = \otimes_{i=x,y,z} \exp \left[ \int_{t_0}^t dt_1 N_i(t_1) + \frac{1}{2} \int_0^t dt_1 \int_0^{t_1} dt_2 [N_i(t_1), N_i(t_2)] + \dots \right] \\ \text{with } N_i(t) = \begin{pmatrix} 0 & 1 \\ \gamma_{ii}(t) & 0 \end{pmatrix} \quad (20)$$

where  $\otimes_{i=x,y,z}$  denotes again a tensor product. This expansion has the advantage to preserve the unitarity of the evolution operator: at any order, the operator obtained by truncating the series in the exponential is unitary. The Magnus expansion can be considered as the continuous generalization of the Baker-Hausdorff formula [41] giving the exponential of a sum of two operators  $A$  and  $B$  as a function of a series of commutators along  $\exp(A + B) = \exp A \exp B \exp([A, B]/2) \dots$ . The Magnus expansion has been successfully applied to solve various physical problems, among which differential equations in classical and quantum mechanics [42], spectral line broadening [43], nuclear magnetic resonance [44], multiple photon absorption [45] and strong field effects in saturation spectroscopy [46].

The first-order term  $\Omega_1(t, t_0)$  in the argument of the exponential can be expressed as

$$\Omega_1(t, t_0) = \int_{t_0}^t dt' N(t') = \begin{pmatrix} 0 & \tau \\ \langle \gamma \rangle \tau & 0 \end{pmatrix} \quad (21)$$

with the duration  $\tau = t - t_0$  and the average quadratic diagonal matrix  $\langle \gamma \rangle_{ii} = 1/\tau \int_{t_0}^t dt \gamma_{ii}(t)$ . Exact expressions for  $\langle \gamma \rangle_{ii}$  are given in Eq. (C1) of Appendix C for a cylindrical condensate. Without this symmetry, the matrix elements  $\langle \gamma \rangle_{ii}$  cannot be evaluated analytically to our knowledge, but are nonetheless accessible with efficient numerical methods [iv]. The first-order ABCD matrix  $M_1^{(1)}(t, t_0, X_0) = e^{\Omega_1(t, t_0)}$  reads [v]:

$$M_1^{(1)} = \begin{pmatrix} \cosh(\langle \gamma \rangle^{1/2} \tau) & \langle \gamma \rangle^{-1/2} \sinh(\langle \gamma \rangle^{1/2} \tau) \\ \langle \gamma \rangle^{1/2} \sinh(\langle \gamma \rangle^{1/2} \tau) & \cosh(\langle \gamma \rangle^{1/2} \tau) \end{pmatrix} \quad (22)$$

[iv] In the short expansion limit considered later where  $|t - t_0| \ll m v_i^2(t_0)/\hbar$ , the average quantities  $\langle \gamma_{ii} \rangle$  can be approximated by the instantaneous value of the quadratic coefficient  $\gamma_{ii}$  at the center of the considered time interval.

[v] For repulsive interactions, all the eigenvalues of the matrix  $\gamma$  are positive, and by convention its square root has also positive eigenvalues.

As expected, this main contribution of the Magnus expansion is independent of the ordering of the successive infinitesimal lenses, and can be interpreted as the ABCD matrix of a thick lens with finite curvature. This expression is similar to the paraxial ABCD matrix obtained in [18] to describe the interactions between an atom laser and a condensate of known wave-function.

In the following developments, we use mainly this first-order contribution to the Magnus expansion. In order to justify this approximation, we have performed a second-order computation of the ABCD matrix  $M^{(1)}(t, t_0, X_0)$  in Appendix B. This second-order correction is weighted by the small parameter  $\epsilon = (\tau/\tau_c)^4$ , depending on the ratio of the duration  $\tau = t - t_0$  to a time-scale  $\tau_c$ , which reads for a spherical cloud of radius  $w_0$ :

$$\tau \ll \tau_c = \left(\frac{w_0}{4\pi a}\right)^{1/6} \frac{mw_0^2}{\hbar} \quad (23)$$

One checks that the first-order expansion is valid for an arbitrary long time ( $\tau_c \rightarrow \infty$ ) as interaction effects vanish ( $a \rightarrow 0$ ). Considering a sample of initial radius  $w_0 = 10 \mu\text{m}$ , and using the s-wave scattering length  $a \simeq 5.7\text{nm}$  of the  $^{87}\text{Rb}$  [18], one obtains  $\tau_c = 0.31 \text{ s}$ . The convergence of the Magnus series is indeed guaranteed when the following inequality is satisfied [41]:

$$N_m = \int_{t_0}^t dt' \|N(t')\| < \ln(2), \quad (24)$$

and our second-order computation gives an additional heuristic indication of convergence for a flight duration  $\tau \ll \tau_c$ .

## V. STABILITY ANALYSIS OF A MATTER-WAVE RESONATOR

In this Section, we apply the method of the ABCD matrix to discuss the propagation of an atomic sample with mean-field repulsive interactions in a matter-wave resonator [47]. The considered resonator involves a series of focusing atomic mirrors. In this system, there is a competition between the transverse sample confinement provided by the mirrors and the expansion induced by the repulsive interactions, which determines the maximum size of the sample during its propagation. In order to keep the sample within the resonator, its transverse size must stay smaller than the diameter of the laser beams realizing the atomic mirrors. If this criterium is met during the successive bounces, the resonator is considered as stable. The ABCD matrix method developed previously, giving an easy derivation of the sample width evolution, is well-suited to discuss this issue. One assumes an initial Gaussian profile for the sample wave-function. The atomic wave propagation in-between the mirrors is treated in the aberrationless approximation, and described by the nonlinear ABCD matrix (22) accounting for self-interaction effects. The evolution of the

sample width obtained with this method is compared to the behavior expected from a non-perturbative paraxial approach.

### A. Resonator description

The considered matter-wave resonator is based on the levitation of a free-falling two-level atomic sample by periodic vertical Raman light pulses. This proposal is described in detail in the reference [47], but we remind here its main features for the sake of clarity. In the absence of light field, the atomic sample propagates in the Hamiltonian (1). We consider an elementary sequence which consists in a pair of two successive short vertical Raman  $\pi$  pulses [4]. Each pulse is performed by two counter-propagating laser beams of respective frequencies  $\omega_{up}$ ,  $\omega_{down}$  and wave-vectors  $k_{up} = k\mathbf{z}$ ,  $k_{down} = -k\mathbf{z}$  equal in norm to a very good approximation and of opposite orientation. The first Raman pulse propagates upward with an effective vertical wave-vector  $\mathbf{k}_{e,1} = 2k\mathbf{z}$  and corresponds to laser frequencies  $\omega_{up} = \omega_2$ ,  $\omega_{down} = \omega_1$ ; the second one propagates downward with an effective vertical wave-vector  $\mathbf{k}_{e,2} = -2k\mathbf{z}$  and with the laser frequencies  $\omega_{up} = \omega_3$  and  $\omega_{down} = \omega_4$ . The frequencies  $\omega_{1,2,3,4}$  are adjusted so that both Raman pulses have the same effective frequency  $\omega_e = |\omega_{up} - \omega_{down}|$ , satisfying the resonance condition [47]  $\omega_e = \omega_2 - \omega_1 = \omega_4 - \omega_3 = \omega_{ba} - 2\hbar k^2/(m\hbar)$ . The intermediate level involved during the Raman pulses (of energy  $E = \hbar(\omega_a + \omega_e)$ ) is taken sufficiently far-detuned from the other atomic energy levels to make spontaneous emission negligible [vi]. After adiabatic elimination of the intermediate level, the action of the Raman pulses can be modelled by the effective dipolar Hamiltonian:

$$\hat{H}_{dip}(t) = -\hbar\Omega_{ba}(\mathbf{r}, t) \cos(\omega_e t - \mathbf{k}_{e,1,2} \cdot \hat{\mathbf{r}}) (|b\rangle\langle a| + |a\rangle\langle b|) \quad (25)$$

Each pair of pulses acts as an atomic mirror, bringing back the atoms in their initial internal state  $a$ , and providing them with a net momentum transfer of  $\Delta\mathbf{p} \simeq 4\hbar\mathbf{k}$ . The atomic motion is sketched on Fig. 1 in the energy-momentum picture.

This sequence can be repeated many times. If the period  $T$  in-between two successive atomic mirrors is set to

$$T := T_0 = \frac{4\hbar k}{mg}, \quad (26)$$

the acceleration provided by the Raman pulses compensates on average that of gravity: the cloud levitates and evolves inside a matter-wave resonator [47]. An analogous system has been realized experimentally recently [49].

---

[vi] In practice, a detuning on the order of the GHz - experimentally compatible with  $\pi$  pulse of duration shorter than the ms [48] - is sufficient to discard spontaneous emission.

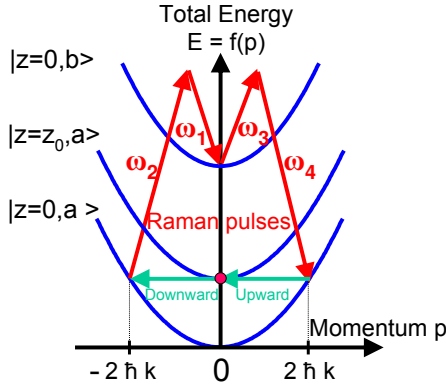


FIG. 1: (Color online) Evolution of the atomic sample in the energy-momentum picture. The total energy includes the kinetic, gravitational and internal energy. The atoms are initially at rest ( $p = 0$ ), at the altitude  $z_0$ , and in the lower state  $a$ . The starting point is thus at the intersection of the paraboloid  $(a, z_0)$  and of the vertical axis ( $p=0$ ). In between the pulses, the motion of the atomic sample in the gravity field is conservative: it corresponds to a leftward horizontal trajectory of the representative point.

### B. Focusing with atomic mirrors.

Matter-wave focusing can be obtained, in principle, with laser waves of quadratic intensity profile [50, 51] or alternatively of spherical wave-front [47]. We concentrate on the focusing obtained with an electric field of quadratic intensity profile [51], the discussion of which is less technical. The Rabi frequency considered for the Raman pulses of the resonator depends quadratically on the distance to the propagation axis  $O_z$  [vii] :

$$\Omega_{ba}(x, y, z, t) = \left(1 - \frac{x^2 + y^2}{2w_{las}^2}\right) \Omega_0(t) \quad (27)$$

These Raman pulses generate a quadratic position-dependent light-shift proportional to the field intensity and thus to the square of the Rabi frequency (27). After the pulse, the atomic wave-function initially in of the form of Eq. (7) is thus multiplied by a factor yielding the input-output relation:

$$\psi_{out}(\mathbf{r}, t) = e^{i2k(z-z_0)} e^{-i(x^2+y^2)/w_{las}^2} e^{i\phi'_0} \psi_{in}(\mathbf{r}, t) \quad (28)$$

with  $\phi'_0$  a constant phase added at the condensate center  $\mathbf{r}_0 = (0, 0, z_0)$  during the pulse. The outgoing wave-function can thus be put again in the form of Eq. (7) if one replaces  $p_0$  by  $p_1 = p_0 + 2\hbar k$ , and  $X_0, Y_0$  with

$$\begin{pmatrix} X_1 \\ Y_1 \end{pmatrix} = \begin{pmatrix} I_3 & 0_3 \\ D(-1/f, -1/f, 0) & I_3 \end{pmatrix} \begin{pmatrix} X_0 \\ Y_0 \end{pmatrix} \quad (29)$$

[vii] Close to the propagation axis, this quadratic profile can be reproduced to a good approximation with Raman pulses of Gaussian intensity profile.

$I_3, 0_3$  are the  $3 \times 3$  identity matrix and null matrix,  $D(-1/f, -1/f, 0)$  is as previously a  $3 \times 3$  diagonal matrix. The focal time is:

$$f = \frac{mw_{las}^2}{2\hbar} \quad (30)$$

Eq. (29) shows that the pulse acts as a lens in the transverse directions  $O_x, O_y$  [viii] .

The strength of the focusing which can be achieved with such atomic mirrors [ix] is indeed limited by the quasi-uniformity required for the Rabi frequency on the condensate surface, in order to perform an efficient population transfer with the Raman  $\pi$ -pulse. Considering a cigar-shaped cloud of small width  $w_\perp$  along the  $O_x, O_y$  axis, one may require that the Rabi frequency difference between the border and the center of the cloud satisfies:  $|\Omega(w_\perp, 0, z, t) - \Omega_0(t)|/|\Omega_0(t)| \leq \epsilon$ . This yields readily a lower bound on the focal time  $f$ :

$$f \geq \frac{mw_\perp^2}{2\hbar\epsilon} \quad (31)$$

With a reasonable bound of  $\epsilon = 10^{-2}$ , a cylindrical cloud of  $^{87}\text{Rb}$  atoms of transverse size  $w_\perp \simeq 10\mu\text{m}$ , one obtains a minimum focusing time:  $f \geq 6.7\text{s}$ . A back-on-the-envelope computation of the reflection coefficient shows that the losses resulting from such an inhomogeneity of the Rabi frequency are on the order of  $10^{-3}$ .

### C. Resonator stability analysis.

We now investigate the non-linear ABCD propagation of a cigar-shaped sample in the resonator. As a specific example, we consider a cloud of  $^{87}\text{Rb}$  atoms taken in the two internal levels  $|a\rangle = |5S_{1/2}, F = 1\rangle$  and  $|b\rangle = |5S_{1/2}, F = 2\rangle$ . In-between the Raman mirrors, the whole sample is expected to propagate in the ground state  $|a\rangle$ . We consider a sample of  $N = 10^5$  atoms, of initial dimensions  $w_x = w_y = w_r = 10\mu\text{m}$  and  $w_z = 100\mu\text{m}$ , and we use the s-wave scattering length  $a \simeq 5.7\text{nm}$  of the Rubidium. We investigate the evolution of this sample during a thousand bounces and for various mirror focal times. Keeping a significant atomic population inside a matter-wave resonator during such a big number of reflections is challenging, but not impossible in principle given the high population transfer which has been achieved experimentally with Raman

[viii] The absence of focusing in the direction of laser beam propagation  $O_z$  is not critical since it does not drive the cloud out of the beam.

[ix] The considered atomic mirrors consist indeed not in a single, but in a double Raman pulse. This does not change the qualitative discussion of this paragraph.

pulses [52] [x]. One obtains the value  $T_0 \simeq 1.5 \text{ ms}$  for the period between the Raman mirrors. This time scale is much shorter than the duration  $\tau_c \simeq 0.3 \text{ s}$  found for the validity of the first-order Magnus expansion associated with a spherical cloud of radius  $w_0 = 10 \mu\text{m}$ . This shows that the ABCD matrix of the cigar-shaped condensate is well-approximated by the leading order [Eq. (22)] of the Magnus expansion [xi]. Furthermore, the free-propagation time  $T_0$  is also much shorter than the time-scale  $\tau_r = mw_r^2/\hbar$  associated with the free expansion of the transverse width, so that one can safely approximate the average quadratic coefficient  $\langle \gamma \rangle$  with the instantaneous value  $\langle \gamma \rangle \simeq \gamma(w_x T_0/2, w_y T_0/2, w_z T_0/2)$ .

To compute the evolution of the transverse and longitudinal sample width, one proceeds as follows. As in Section IV A, one starts with initial width matrices  $X_0 = iD(w_{x0}, w_{y0}, w_{z0})$  and  $Y_0 = \frac{\hbar}{m}D(1/w_{x0}, 1/w_{y0}, 1/w_{z0})$  and computes the interacting ABCD matrix (22) as a function of these initial widths. During the first cycle, one multiplies the corresponding vector  $(X_0, Y_0)$  successively with nonlinear ABCD matrix (22) and with the mirror ABCD matrix (29). The new width matrices  $(X_1, Y_1)$  are obtained, from which one can infer the nonlinear ABCD matrix for the next propagation stage. The iteration of these algebraic operations is a straightforward numerical task. The results, depicted on Fig. 2, show that the transverse width oscillates with an amplitude and a period which both increase with the mirror focal time. The maximum sample size is  $w_r = 25 \mu\text{m}$  and  $w_r = 60 \mu\text{m}$  for the respective focal times  $f = 20 \text{ s}$  and  $f = 100 \text{ s}$ . Considering for instance a laser beam of waist  $w = 100 \mu\text{m}$  in the experiment, one sees that with those focal times the atomic cloud remains within the light beam and is thus efficiently confined transversally in the resonator. As expected, the use of Raman mirrors with a stronger curvature allows one to shrink the transverse size of the stabilized cloud. Fig. 3 shows the evolution of the maximum sample transverse size as a function of the mirror focal time. The extended ABCD matrix

analysis presented in this paper allows thus to determine efficiently the minimum amount of focusing required to keep the sample within the diameter of the considered Raman lasers. In that respect it can be used to optimize the trade-off, exposed in the previous paragraph, between strongly focusing or highly reflecting atomic mirrors.

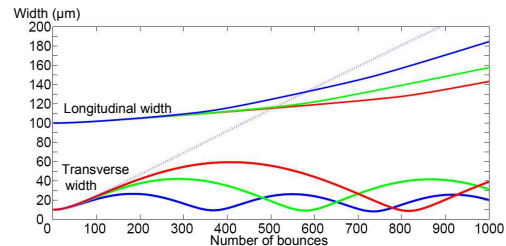


FIG. 2: (Color online) Evolution of the transverse and longitudinal width of the sample ( $\mu\text{m}$ ) during the successive bounces in the cavity (numbered from 1 to 1000), for the mirror focal times  $f = 20 \text{ s}$  (blue),  $f = 50 \text{ s}$  (green) and  $f = 100 \text{ s}$  (red). The dashed line represents the evolution of the transverse width in the absence of focusing with the Raman mirrors.

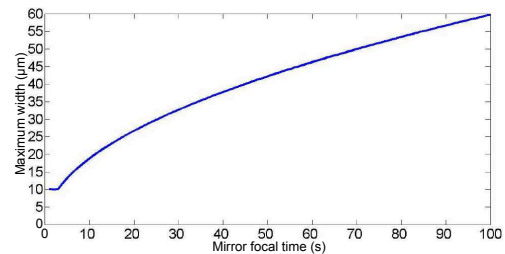


FIG. 3: (Color online) Maximum sample transverse width ( $\mu\text{m}$ ) during the evolution in the resonator as a function of the Raman mirror focal time (s). We have considered the first 1000 bounces to determine this maximum.

#### D. Comparison with the predictions of the nonlinear paraxial equation.

As exposed in Appendix A, the propagation of an atomic beam with a longitudinal momentum much greater than the transverse momenta can be alternatively described by a paraxial wave equation of the form (A2). Furthermore, if the linear density of the atomic beam is uniform, the nonlinear coefficient intervening in this paraxial equation is a constant. As in nonlinear optics [53] and in 2D condensates [54], this equation induces a universal behavior in paraxial atomic beams [55]: the transverse width oscillates with a frequency independent from the strength of the interaction. The width oscillations, depicted on Fig. 2, indeed allow one to confront the results of our method,

[x] We treat the wave-propagation in the resonator as if the atomic cloud was entirely reflected on the successive atomic mirrors. Indeed, even if resonant Raman pulses can perform a population transfer with an efficiency close to 99% [52], the residual losses become significant after a big number of bounces in a real experiment. This results in a gradual decrease of the mean-field interactions, which could be accounted for in a more sophisticated model. Our point here is simply to illustrate the nonlinear ABCD method on a thought experiment, and we thus adopted a simplified approach with perfect atomic mirrors.

[xi] We have computed the time-scale  $\tau_c$  determining the validity of the first-order Magnus term for spherical wave-packets only. Nonetheless, a basic dimensional analysis shows that for a cigar-shaped cloud, the time-scale determining the validity of the first-order Magnus term is bounded below by the time  $\tau_c$  given by Eq. (23) and computed by setting  $w_0$  equal to the smallest cigar dimension.



which uses a non-paraxial wave equation treated in the aberrationless approximation, to the predictions of the full nonlinear paraxial equation with a uniform nonlinear coefficient. We stress that this second approach leaves the nonlinear term as such and does not assume that the Gaussian shape of the atomic beam is preserved. In this sense it is more exact than the radius of curvature method used in Appendix A. It is also approximate, since the atomic beam is neither paraxial nor of uniform linear density. Nevertheless, it is remarkable that both treatments agree very well on the oscillation period of the width.

To apply the paraxial description, one models the action of the successive mirrors on the transverse wave-function with an average potential. The lens operated by each Raman mirror, of focal time  $f$ , imprints a phase factor of  $e^{i\frac{m}{2\hbar T}r^2}$  [see Eq. (28) and Eq. (30)]. The series of lenses, separated by the duration  $T_0$ , thus mimics the following effective quadratic potential:

$$V_{\perp, lens} = \frac{m}{2\hbar^2 T_0 f} r^2 \quad (32)$$

Let us consider the nonlinear contribution, given by a contact term of the form  $V_{\perp, int}(\mathbf{r}) = g_I |\psi_{//}(z)|^2 |\psi_{\perp}(\mathbf{r})|^2 \psi_{\perp}(\mathbf{r})$ , with  $\psi_{//}(z)$  the longitudinal wave-function [Eq. (A1) of Appendix A]. The term  $g_I |\psi_{//}(z)|^2$  appears as an effective nonlinear coupling coefficient for the transverse wave-function depending on the altitude  $z$ . Adding this nonlinear contribution to Eq. (A1), one obtains a 2D nonlinear Schrödinger equation (NLSE):

$$i\hbar\partial_{\zeta}\psi_{\perp}(x, y, \zeta) = \left[ -\frac{\hbar^2}{2m}(\partial_x^2 + \partial_y^2) + g_I |\psi_{//}(\zeta)|^2 |\psi_{\perp}|^2 + \frac{m}{2\hbar^2 T_0 f} r^2 \right] \psi_{\perp}(x, y, \zeta), \quad (33)$$

$\zeta$  is a parameter defined in Eq. (A1) equivalent to the propagation time,  $a$  the scattering length and  $r^2 = x^2 + y^2$ . Setting  $K = \frac{m}{\hbar}$ , one can recast this equation in the same form as in [53] where the propagation of a light wave in a quadratic graded index medium was considered:

$$2iK\partial_{\zeta}\psi_{\perp} = \left[ -\partial_T^2 + (8\pi a |\psi_{//}|^2) |\psi_{\perp}|^2 + K^2 \left( \frac{1}{fT_0} \right) r^2 \right] \psi_{\perp}, \quad (34)$$

We now make the assumption that the variations of the non-linear coefficient  $8\pi a |\psi_{//}(\zeta)|^2$  with  $\zeta$  are sufficiently smooth to have a negligible impact on the period of the sample width oscillations. This assumption seems reasonable for the considered cigar-shaped cloud, which has a slow longitudinal expansion in comparison with the oscillation period [see Fig. 2]. This hypothesis is indeed validated *a posteriori*, since it leads to predictions in excellent agreement with the results of the ABCD method discussed above. Once the nonlinear coefficient is approximated with a constant, one can readily apply the results

derived in [53, 55], which show that Eq. (34) yields transverse oscillations of universal frequency:

$$\omega_{par} = \frac{2}{\sqrt{fT_0}} \quad (35)$$

The results obtained from the perturbative ABCD approach are confronted with this prediction on Fig. 4. The agreement improves as the mirror focal time increases, and it is in fact already good (4%) for a focal time of  $f = 3$  s and attains 0.7% for a focal time of  $f = 50$  s. As discussed above, focal times shorter than  $f = 20$  s seem incompatible with the reflection coefficient desired for the atomic mirrors. The disagreement observed below  $f \leq 3$  s may be attributed to a failure of the paraxial approximation to describe the propagation of the sample in our system.

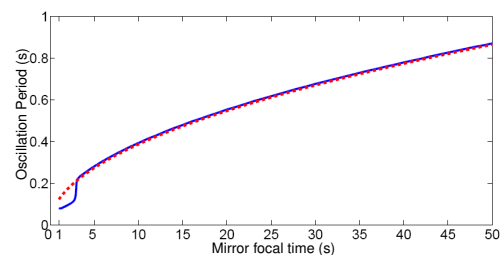


FIG. 4: (Color online) Period of the transverse width oscillations (s) in the matter-wave resonator as a function of the Raman mirror focal time (s). The full and the dashed line give the oscillation periods obtained respectively through the perturbative ABCD approach and through the nonlinear paraxial wave equation.

## VI. CONCLUSION

This paper exposed a treatment of the non-linear Schrödinger equation involving theoretical tools from optics and atom-optics. The ABCD propagation method for matter waves has been extended beyond the linear regime thanks to a perturbative analysis relying on an atom-optical aberrationless approximation. We have derived approximate analytical expressions for the ABCD matrix of an interacting atomic cloud thanks to a Magnus expansion. This matrix analysis has been applied to discuss the propagation of an atomic sample in a perfect matter-wave resonator. We have shown that such sample can be efficiently stabilized thanks to focusing atomic mirrors. We have found that the nonlinear ABCD propagation reproduces to a good level of accuracy the universal oscillations expected from the nonlinear paraxial equation for matter waves [55], which makes it a promising tool to model future nonlinear atom optics experiments and a seducing alternative to previous numerical methods applied to matter-wave resonators [50]. We

have also highlighted an other optical method, involving more stringent assumptions - paraxial propagation, cylindrical symmetry and constant longitudinal velocity - and also relying on the aberrationless approximation. This last method enables one to address self-interaction effects in the free propagation through a complex parameter [defined in Eq. (A13)], which is analogous to a radius of curvature, and the evolution of which is very simple [Eq. (A14)]. As far as the beam width is concerned, the effect of self-interactions can be interpreted as a scaling transformation of the free propagation by a factor depending on the matter-wave flux  $\mathcal{F}$  [See Eq. (A15)]. Both approaches are relevant to study interaction effects on the stability of atomic sensors resting on Bloch oscillations [56], on the sample propagation in coherent interferometers [57]. An interesting continuation of this work would be to develop a nonlinear ABCD matrix analysis beyond the aberrationless approximation.

### ACKNOWLEDGEMENTS

The authors acknowledge enlightening discussions with Yann Le Coq on the nonlinear paraxial equation for matter waves. François Impens thanks Nicim Zagury and Luiz Davidovich for their hospitality. This work was supported by DGA (Contract No 0860003) and by CNRS. Our research teams in SYRTE and Laboratoire de Physique des Lasers are members of IFRAF(www.ifraf.org).

### APPENDIX A: THE METHOD OF THE NON-LINEAR RADIUS OF CURVATURE.

This method addresses the paraxial propagation of a monochromatic and cylindrical matter-wave beam. It relies on the introduction of an effective complex radius of curvature [23, 26], which evolution is especially simple, even for a self-interacting beam. It has been applied successfully by Bélanger and Paré [24] to describe self focusing phenomena of cylindrical optical beams propagating in the paraxial approximation, and it works equally well for matter waves propagating in the same regime. This is typically the case for an atom laser beam falling into the gravity field, for which the transverse momentum components become negligible compared to the vertical momentum after sufficient time [18].

We consider a mono-energetic wave-packet propagating in the paraxial regime, and evolving in the sum of a longitudinal potential  $V_{//}(z)$  and a transverse one  $V_{\perp}(x, y, z)$ , which may also vary slowly with the longitudinal coordinate  $z$ . This section begins with a brief remainder on the paraxial equation for matter waves [33], and on its spherical-wave solutions in the linear case [23]. It is remarkable that such solutions can be extended to

the nonlinear propagation [23], at the cost of certain approximations, and thanks to the introduction of a generalized radius of curvature depending on the coupling strength. Our treatment of the nonlinear matter wave propagation follows step by step the approach of Bélanger and Paré for optical waves [24].

#### 1. The Paraxial Equation for Matter Waves.

Our derivation of the nonlinear paraxial wave-equation follows the treatment done in [33]. The wave-function is factorized into a transverse and longitudinal component:

$$\psi(x, y, z) = \psi_{\perp}(x, y, z) \psi_{//}(z)$$

The longitudinal component obeys a 1D time-independent Schrödinger equation,

$$-\frac{\hbar^2}{2m} \frac{\partial^2 \psi_{//}}{\partial z^2} + V_{//} \psi_{//} = E \psi_{//},$$

which can be solved with the WKB method:

$$\psi_{//}(z) = \sqrt{\frac{m\mathcal{F}}{p(z)}} \exp\left[\frac{i}{\hbar} \int_{z_0}^z du p(u)\right].$$

$\mathcal{F} = \int d^2\mathbf{r}_{\perp} \frac{p(z)}{m} |\psi(\mathbf{r}_{\perp}, z)|^2$  is the atomic flux evaluated through any infinite transverse plane, the transverse wave-function  $\psi_{\perp}$  being normalized to unity  $\int d^2\mathbf{r}_{\perp} |\psi_{\perp}(\mathbf{r}_{\perp}, z)|^2 = 1$ .  $p(z) = \sqrt{2m(E - V_{//}(z))}$  is the classical momentum along  $z$ , and  $z_0$  is the associated classical turning point verifying  $p(z_0) = 0$ . The transverse wave-function  $\psi_{\perp}$ , assumed to depend slowly enough on the coordinate  $z$  to make its second derivative negligible, verifies the equation:

$$\left[ i\hbar \frac{p(z)}{m} \partial_z + \frac{\hbar^2}{2m} (\partial_x^2 + \partial_y^2) - V_{\perp}(x, y, z) \right] \psi_{\perp}(x, y, z) = 0.$$

This equation can be simplified with a variable change in which the longitudinal coordinate  $z$  is replaced by the parameter  $\zeta$ :

$$\zeta(z) = \int_{z_0}^z dz \frac{m}{p(z)} \quad (\text{A1})$$

which corresponds to the time needed classically to propagate from the turning point  $z_0$  to the coordinate  $z$  [xii]. The wave equation becomes

$$\left[ i\hbar \partial_{\zeta} + \frac{\hbar^2}{2m} (\partial_x^2 + \partial_y^2) - V_{\perp}(x, y, \zeta) \right] \psi_{\perp}(x, y, \zeta) = 0, \quad (\text{A2})$$

---

[xii] Indeed, this parameter appear as proportional to the proper time experienced by the atom on the classical trajectory determined by  $p(z)$  [59].

We assume from now on that the transverse potential  $V_{\perp}(x, y, z)$  has a cylindrical symmetry. If one sets  $K = m/\hbar$  and  $V_{\perp}(x, y, \zeta) = \frac{\hbar}{2}K_2(\zeta)r^2$  with  $r^2 = x^2 + y^2$ , Eq. (A2) has the same form as the paraxial equation for the electric field used in [24]:

$$\left[\partial_T^2 + 2iK\partial_{\zeta} - KK_2(\zeta)r^2\right]\psi_{\perp}(x, y, \zeta) = 0, \quad (\text{A3})$$

It is worth noticing that, as a consequence of our variable change, the derivative with respect to the longitudinal coordinate  $z$  has been replaced by a time derivative with respect to  $\zeta$ .

## 2. Spherical Wave solutions to the linear equation.

One looks for solutions of Eq. (A3) of the kind:

$$\psi_{\perp}(x, y, \zeta) = A(\zeta) \exp\left[i\frac{K}{2q(\zeta)}r^2\right] \quad (\text{A4})$$

with again  $K = m/\hbar$ . Such function is a solution if and only if the parameter  $q(\zeta)$  - called complex radius of curvature, and homogenous to a time for matter waves - satisfies the following equation:

$$\frac{q' - 1}{q^2} - \frac{K_2(\zeta)}{K} = 0 \quad (\text{A5})$$

and if the amplitude  $A(\zeta)$  verifies:

$$\frac{A'}{A} + \frac{1}{q} = 0 \quad (\text{A6})$$

The prime stands for the derivative with respect to  $\zeta$ . In the absence of the transverse potential, i.e.  $V_{\perp}(x, y, \zeta) = 0$ , an obvious evolution is obtained with  $q(\zeta) = \zeta$ .

These equations imply a relation between the amplitude and width of the wave-function. We adopt the usual decomposition for the complex radius of curvature along its imaginary and complex part:

$$\frac{1}{q} = \frac{1}{R} + \frac{2i}{Kw^2}$$

Assuming that  $K_2(\zeta)$  is real, and combining the imaginary part of Eq. (A5) with the real part of Eq. (A6), one obtains:

$$|A(\zeta)|^2 = |A_0|^2 \frac{w_0^2}{w^2(\zeta)}$$

This relation reflects the conservation of the atomic flux  $\mathcal{F}$  along the propagation. With our choice of normalization, the parameter  $|A|^2$  is given by:

$$|A|^2 = \frac{2}{\pi w^2} \quad (\text{A7})$$

## 3. Spherical Wave solutions to the nonlinear equation.

With several approximations, it is possible to find similar solutions in the interacting case. Atomic interactions are described by the mean-field potential

$$V_i(x, y, \zeta) = g_I^0 |\psi_{//}(z)|^2 |\psi_{\perp}(x, y, \zeta)|^2 \quad \text{with} \quad g_I^0 = \frac{4\pi\hbar^2 a}{m}$$

which intervenes in the time-independent equation verified by  $\psi$ . Because we adopt here a different normalisation for the wave-function, the nonlinear coupling constant  $g_I^0$  differs from the coupling constant  $g_I$  used previously:  $g_I^0 = g_I/N$ . The mean-field contribution induces the following transverse potential

$$V_{\perp}(x, y, \zeta) = g_I^0 |\psi_{//}(\zeta)|^2 (|\psi_{\perp}(x, y, \zeta)|^2 - |\psi_{\perp}(0, 0, \zeta)|^2)$$

in the paraxial equation verified by  $\psi_{\perp}$ . In the considered example, this potential receives no other contribution. The subsequent analysis requires three important approximations. First, it uses the ‘‘aberrationless approximation’’, which assumes that the wave-function follows the Gaussian profile (A4) in spite of the non-linearity. Second, it assumes that the transverse mean-field potential is well-described by a second order expansion,

$$V_{\perp}(x, y, \zeta) \simeq -2g_I^0 |\psi_{//}(\zeta)|^2 \frac{|A(\zeta)|^2}{w^2(\zeta)} r^2 \quad (\text{A8})$$

The term  $G(\zeta) = g_I^0 |\psi_{//}(\zeta)|^2$  can be seen as the atom-optical equivalent of a third-order non-linear permittivity. Third, it neglects the dependence on  $G(\zeta)$  towards the altitude, which is a valid approach if the linear density  $n_{1D} = m\mathcal{F}/p(z)$  is a constant [xiii]. We assume from now on that the atomic flux  $\mathcal{F}$  is constant and that the average longitudinal momentum  $p(z) = \sqrt{2m(E - V_{//}(z))} \simeq p_{0//}$  varies very slowly with  $z$ . The parameter  $\zeta$  can then be expressed simply as  $\zeta = m(z - z_0)/p_{0//}$ . Eq. (A8) and the normalization of  $\psi_{\perp}$  [Eq. (A7)] give readily:

$$\frac{K_2(\zeta)}{K} = \frac{-8g_I^0 \mathcal{F}}{\pi p_{0//} w^4(\zeta)}$$

Eq. (A5) can then be recast as:

$$\frac{q' - 1}{q^2} + \frac{\mathcal{F}}{\mathcal{F}_c} \left( \frac{4}{K^2 w^4(\zeta)} \right) = 0$$

The quantity  $\mathcal{F}_c$ , called critical flux, reads  $\mathcal{F}_c = \pi p_{0//} \hbar^2 / (2g_I^0 m^2)$ . The last equation may be split into its real and imaginary part along:

$$\left(\frac{1}{R}\right)' + \frac{1}{R^2} - \sigma \left(\frac{2}{Kw^2}\right)^2 = 0 \quad (\text{A9})$$

---

[xiii] This approximation is indeed implicit in the treatment of Bélanger and Paré [24], since it is necessary to obtain the nonlinear paraxial wave-equation which is the starting point of their analysis.

and

$$\left(\frac{1}{Kw^2}\right)' + 2\left(\frac{1}{R}\right)\left(\frac{2}{Kw^2}\right) = 0 \quad (\text{A10})$$

where we have introduced the dimensionless parameter  $\sigma = 1 + \mathcal{F}/\mathcal{F}_c$ . This system can be uncoupled thanks to the following trick: Eq. (A10) is multiplied by  $i\sqrt{\sigma}$  and added to Eq. (A9). One obtains:

$$\left(\frac{1}{R}\right)' + i\sqrt{\sigma}\left(\frac{2}{Kw^2}\right)' + \frac{1}{R^2} + \frac{2i\sqrt{\sigma}}{R}\left(\frac{2}{Kw^2}\right) - \sigma\left(\frac{2}{Kw^2}\right)^2 = 0 \quad (\text{A11})$$

This equation can be simply interpreted as

$$q'_{NL} - 1 = 0 \quad (\text{A12})$$

with the generalized complex radius of curvature:

$$q_{NL} = \frac{1}{R} + \frac{2\sqrt{\sigma}i}{Kw^2} \quad (\text{A13})$$

Its very simple evolution

$$q_{NL}(z) = q_{NL}(z_0) + \frac{m(z - z_0)}{p_{0//}} \quad (\text{A14})$$

gives readily the real radius of curvature  $R(z)$  and the width  $w(z)$  for any altitude  $z$ . One thus has, as in the linear case, a simple spherical-wave solution (A4). Indeed, this method allows one to approximate very efficiently the nonlinear propagation of a wave-function of initial Gaussian profile. Consider a Gaussian atomic beam of width  $w(z_0) = w_0$  at the waist ( $R(z_0) = +\infty$ ) situated at the position  $z_0$  on the propagation axis. Eqs. (A13) and (A14) show that the beam width follows:

$$w(z) = \sqrt{w_0^2 + \frac{\hbar^2}{w_0^2 p_{0//}^2} \sigma (z - z_0)^2} \quad (\text{A15})$$

The width of a self-interacting atomic beam evolves thus as an interaction-free beam in which the propagation length from the waist is multiplied by a factor  $\sqrt{\sigma}$ . As far as the paraxial beam width evolution is concerned, self-interaction effects thus operate as a scaling transformation of the free propagation with a factor  $\sqrt{\sigma}$ . The quantity  $\sqrt{\sigma} - 1$  has the same sign as the scattering length  $a$ , so one checks that Eq. (A15) leads consistently to a faster expansion for repulsive interactions and to a slower expansion for attractive ones. As in optics, this treatment can thus be applied to discuss the self focusing

for matter waves. It is, however, important to keep in mind its validity domain and the several hypothesis required - constant longitudinal velocity, cylindrical symmetry, paraxial propagation and Gaussian shape approximation -. Last, we point out the independent work of Chen *et. al.* [58] on this nonlinear radius of curvature.

## APPENDIX B: SECOND-ORDER COMPUTATION OF THE NONLINEAR ABCD MATRIX.

### 1. Expression of the second-order matrix.

In this Appendix, we discuss the nonlinear corrections to the ABCD matrix associated with the second-order term of the Magnus expansion  $\Omega_2(t, t_0) = \frac{1}{2} \int_{t_0}^t dt_1 \int_{t_0}^{t_1} dt_2 [N(t_1), N(t_2)]$ , which reads:

$$\Omega_2(t, t_0) = \begin{pmatrix} S(t, t_0) & 0 \\ 0 & -S(t, t_0) \end{pmatrix}$$

$$\text{with } S(t) = \int_{t_0}^t dt_1 \int_{t_0}^{t_1} dt_2 (\gamma(t_1) - \gamma(t_2)) \quad (\text{B1})$$

This term, arising from the non-commutativity between the Hamiltonians taken at different times, naturally depends on the ordering chosen for the successive lenses. Because of the cloud expansion, lenses are ordered from the most divergent to the less divergent. To discuss the effect of this second-order contribution on the wave-function, it is useful to compute the exponential:

$$\exp[\Omega^{(2)}(t, t_0)] = \begin{pmatrix} e^{S(t, t_0)} & 0 \\ 0 & e^{-S(t, t_0)} \end{pmatrix} \quad (\text{B2})$$

The action of such matrix onto the position-momentum width vector  $(X, Y)$ , defined in Sec. III A, would operate a squeezing between position and momentum. This squeezing is indeed a consequence of our aberrationless approximation, in which the propagation leaves the phase-space volume invariant: the expansion of the cloud size must be, in our treatment, compensated by a reduced momentum dispersion. One finds consistently that the diagonal matrix elements  $S_{xx,yy,zz}(t)$ , involved in (B2), are positive, which results from the decrease of the matrix elements  $\gamma_{xx,yy,zz}(t)$  with time.

The ABCD matrix obtained from a second-order approximation of the Magnus expansion reads:

$$M_2^{(1)}(t, t_0, X_0) \simeq \otimes_{i=x,y,z} \begin{pmatrix} \cosh K_{ii}(t, t_0) + S_{ii}(t, t_0) \frac{\sinh K_{ii}(t, t_0)}{K_{ii}(t, t_0)} & (t - t_0) \frac{\sinh K_{ii}(t, t_0)}{K_{ii}(t, t_0)} \\ \langle \gamma \rangle \frac{\sinh K_{ii}(t, t_0)}{K_{ii}(t, t_0)} & \cosh K_{ii}(t, t_0) - S_{ii}(t, t_0) \frac{\sinh K_{ii}(t, t_0)}{K_{ii}(t, t_0)} \end{pmatrix} \quad (\text{B3})$$

We have introduced the functions  $K_{ii}(t, t_0) = \sqrt{S_{ii}^2(t, t_0) + \langle \gamma_{ii} \rangle (t - t_0)^2}$ . An analytic expression of  $\langle \gamma_{ii} \rangle$  can

be found for cigar-shaped condensates in Eq. (C1) of Appendix C. The computation of the quantity  $S_{ii}(t, t_0)$  is straightforward, but it involves tedious algebra. Higher-order contributions to the ABCD matrix (20) involve various integrations which need to be performed numerically.

## 2. Comparison with the first-order matrix.

Let us expand the matrix (B7) in the short duration limit. We consider an atomic cloud initially described by a Gaussian wave-function (10) of spherical symmetry i.e.  $w_{x0} = w_{y0} = w_{z0} = w_0$ . Such assumption does not change the nature of the discussion, but it considerably simplifies the algebra: the  $3 \times 3$  matrices  $\gamma(t)$ ,  $S(t)$  and  $K(t)$  are then proportional to the matrix identity  $I_3$  and can be identified to scalars.  $\gamma(t)$  can be expressed as a function of two time scales  $\tau_1, \tau_2$  involving the sample radius  $w_0$ , the scattering length  $a$  and fundamental constants:

$$\gamma(t) = \tau_2^{-2} \left( 1 + \frac{(t - t_0)^2}{\tau_1^2} \right)^{-5/2}, \quad \tau_1 = \frac{mw_0^2}{\hbar}, \quad \tau_2 = \sqrt{\frac{w_0}{4\pi a}} \tau_1 \quad (\text{B4})$$

The quantity  $S(t)$  (B1) can be expressed thanks to a second-order Taylor expansion of  $\gamma(t)$ . Setting  $\tau = t - t_0$  and noticing that  $\gamma'(t_0) = 0$ , one obtains:

$$S(t) = -\frac{5}{6} \frac{\tau^4}{\tau_1^2 \tau_2^2} + O(\tau^6) \quad (\text{B5})$$

which yields for the quantity  $K(t)$ :

$$K(t) = \sqrt{\langle \gamma \rangle} \tau \left( 1 + \frac{25}{72} \frac{\tau^6}{\tau_1^4 \tau_2^2} \right) + O(\tau^8) \quad (\text{B6})$$

Using this expansion and that of  $x \rightarrow \sinh x/x$ , one can express the second-order matrix  $M_2^{(1)}(\tau, X_0)$  as:

$$M_2^{(1)}(\tau, X_0) = M_1^{(1)}(\tau, X_0) + \left( \begin{array}{cc} -\frac{5}{6} \frac{\tau^4}{\tau_1^2 \tau_2^2} \frac{\sinh(\langle \gamma \rangle^{1/2} \tau)}{\langle \gamma \rangle^{1/2} \tau} & \frac{25}{72} \frac{\tau^6}{\tau_1^4 \tau_2^2} \left( \cosh(\langle \gamma \rangle^{1/2} \tau) - \frac{\sinh(\langle \gamma \rangle^{1/2} \tau)}{\langle \gamma \rangle^{1/2} \tau} \right) \\ \frac{25}{72} \frac{\tau^6}{\tau_1^4 \tau_2^2} \left( \cosh(\langle \gamma \rangle^{1/2} \tau) - \frac{\sinh(\langle \gamma \rangle^{1/2} \tau)}{\langle \gamma \rangle^{1/2} \tau} \right) & \frac{5}{6} \frac{\tau^4}{\tau_1^2 \tau_2^2} \frac{\sinh(\langle \gamma \rangle^{1/2} \tau)}{\langle \gamma \rangle^{1/2} \tau} \end{array} \right) + O(\tau^8) \quad (\text{B7})$$

This expansion shows that the first-order term is a valid approximation as long as:

$$\tau \ll \tau_c = \left( \frac{w_0}{4\pi a} \right)^{1/6} \frac{mw_0^2}{\hbar} \quad (\text{B8})$$

Considering for an instance an initial cloud size of  $w_0 = 25 \mu\text{m}$  and the  $^{87}\text{Rb}$  scattering length  $a = 5,7\text{nm}$ , one obtains  $\tau_1 = 0,14\text{s}$ ,  $\tau_2 = 1,63\text{s}$ , and  $\tau_c = 0,31\text{s}$ . Note that the relevant small parameter  $\epsilon$ , weighting the relative correction brought by the second-order term, decreases as  $\epsilon = (\tau/\tau_c)^4$  when  $\tau/\tau_c \rightarrow 0$ .

## APPENDIX C: ABCD MATRIX ELEMENTS FOR THE CIGAR-SHAPED CONDENSATE

We evaluate in this appendix various primitives necessary to explicit the non-linear ABCD matrix to first order in the Magnus expansion given in Eq. (22). We consider a cigar-shaped cylindrical condensate with a long vertical extension:  $w_x = w_y = w_r \ll w_z$ . We remind the linear evolution of the width given by Eq. (11) i.e.  $w_{r,z,t} = \sqrt{w_{r,z,0}^2 + \Delta v_{r,z,0}^2 (t - t_0)^2}$ . We use the short-hand notation  $\Delta v_{r,z,0} = \hbar/(mw_{r,z,0})$ .

We seek to evaluate the average  $\langle \gamma \rangle_{ii} = 1/\tau \int_{t_0}^t dt \gamma_{ii}(t)$  of the time-dependent coefficients:

$$\gamma_{rr}(t) = \frac{\gamma_0}{w_{zt} w_{rt}^4}, \quad \gamma_{zz}(t) = \frac{\gamma_0}{w_{zt}^3 w_{rt}^2}$$

with  $\gamma_0 = g_I / ((2\pi)^{3/2} m)$ . These quantities are readily obtained:

$$\begin{aligned} \langle \gamma_{rr} \rangle &= \gamma_0 \left[ \frac{\Delta v_{r0}^2 w_{zt}}{2w_{r0}^2(\Delta v_{r0}^2 w_{z0}^2 - w_{r0}^2 \Delta v_{z0}^2) w_{rt}^2} + \frac{(\Delta v_{r0}^2 w_{z0}^2 - 2w_{r0}^2 \Delta v_{z0}^2) \text{Arctan } \Lambda(t)}{2w_{r0}^3(\Delta v_{r0}^2 w_{z0}^2 - w_{r0}^2 \Delta v_{z0}^2)^{3/2}(t-t_0)} \right] \\ \langle \gamma_{zz} \rangle &= \gamma_0 \left[ \frac{\Delta v_{z0}^2}{w_{z0}^2(\Delta v_{z0}^2 w_{r0}^2 - \Delta v_{r0}^2 w_{z0}^2) w_{zt}} + \frac{\Delta v_{r0}^2 \text{Arctan } \Lambda(t)}{w_{r0}(\Delta v_{r0}^2 w_{z0}^2 - w_{r0}^2 \Delta v_{z0}^2)^{3/2}(t-t_0)} \right] \\ \text{with } \Lambda(t) &= \frac{\sqrt{\Delta v_{r0}^2 w_{z0}^2 - w_{r0}^2 \Delta v_{z0}^2}(t-t_0)}{w_{rt} w_{zt}} \end{aligned} \quad (C1)$$

- 
- [1] C. J. Bordé, Propagation of Laser Beams and of Atomic systems, in *Fundamental Systems in Quantum Optics*, Les Houches Lectures Session LIII (Elsevier, 1991).
- [2] G. Lenz, P. Meystre, and E. M. Wright, Phys. Rev. Lett. **71**, 3271 (1993).
- [3] W. Zhang and D. F. Walls, Phys. Rev. A **49**, 3799 (1994).
- [4] P. Berman, *Atom Interferometry* (Academic Press, 1997).
- [5] K. V. Krutitsky, F. Burgbacher, and J. Audretsch, Phys. Rev. A **59**, 1517 (1999); K. V. Krutitsky, K.-P. Marzlin, and J. Audretsch, Phys. Rev. A **65**, 063609 (2002).
- [6] L. Deng *et al.*, Phys. Rev. Lett. **83**, 5407 (1999).
- [7] G.-B. Jo *et al.*, Phys. Rev. Lett. **99**, 240406 (2007).
- [8] I. Josopait *et al.*, Eur. Phys. J. D **22**, 385 (2003).
- [9] L. Deng *et al.*, Nature **398**, 218 (1999).
- [10] S. Burger *et al.*, Phys. Rev. Lett. **83**, 5198 (1999).
- [11] J. Denschlag *et al.*, Science **287**, 97 (2000).
- [12] L. Khaykovich *et al.*, Science **17**, 1290 (2002).
- [13] K. E. Strecker, G. B. Partridge, A. G. Truscott, and R. G. Hulet, Nature **417**, 150 (2002).
- [14] M. R. Matthews *et al.*, Phys. Rev. Lett. **83**, 2498 (1999).
- [15] K. W. Madison, F. Chevy, W. Wohlleben, and J. Dalibard, Phys. Rev. Lett. **84**, 806 (2000).
- [16] S. Inouye *et al.*, Science **285**, 571 (1999).
- [17] S. Inouye *et al.*, Nature **402**, 641 (December 1999).
- [18] Y. LeCoq *et al.*, Phys. Rev. Lett. **87**, 170403 (2001).
- [19] T. Busch, M. Köhl, T. Esslinger, and K. Mølmer, Phys. Rev. A **65**, 043615 (2002).
- [20] Y. Castin and R. Dum, Phys. Rev. Lett. **77**, 5315 (1996).
- [21] H. Michinel, Pure Appl. Opt. 701-708 **4**, 701 (1995).
- [22] D. Guéry-Odelin, F. Zambelli, J. Dalibard, and S. Stringari, Phys. Rev. A **60**, 4851 (1999); D. Guéry-Odelin, *Peyresq Lectures on Nonlinear Phenomena*, Vol. II, edited by J-A Sepulchre (World Scientific, Singapore, 2003).
- [23] A. Yariv and P. Yeh, Optics Communications **27**, 295 (1978).
- [24] P.-A. Bélanger and C. Paré, Applied Optics **22**, 1293 (1983).
- [25] C. J. Bordé, Metrologia **39**, 435 (2002).
- [26] H. Kogelnik, Bell System Technical Journal **44**, 455 (1965).
- [27] B. K. Garside, IEEE Journal of Quantum Electronics **4**, 940 (1968).
- [28] A. Le Floch, R. Le Naour, J. M. Lenormand, and J. P. Taché, Phys. Rev. Lett. **45**, 544 (1980).
- [29] F. Bretenaker, A. Le Floch, and J. P. Taché, Phys. Rev. A **41**, 3792 (1990).
- [30] F. Bretenaker and A. Le Floch, Phys. Rev. A **42**, 5561 (1990).
- [31] V. Magni, G. Cerullo, and S. D. Silvestri, Opt. Commun. **96**, 348 (1993).
- [32] J.-F. Riou *et al.*, Phys. Rev. Lett. **96**, 070404 (2006).
- [33] J.-F. Riou *et al.*, Phys. Rev. A **77**, 033630 (2008).
- [34] M. Peskin and D. Schroeder, *An Introduction to Quantum Field Theory* (Addison-Wesley Advanced Book Program, 1995).
- [35] C. J. Bordé, C. R. Acad. Sci. Paris **4**, 509 (2001).
- [36] C. J. Bordé, J.-C. Houard, and A. Karasiewicz, in *Gyros, Clocks and Interferometers: Testing relativistic gravity in space* (Springer-Verlag, 2000), e-print arXiv:gr-qc/0008033.
- [37] C. J. Bordé, General Relativity and Gravitation **36**, 475 (2004).
- [38] F. Impens, Phys. Rev. A **77**, 013619 (2008).
- [39] S. Nemoto, Appl. Opt. **34**, 6123 (1995).
- [40] W. Magnus, Comm. Pure Appl. Math **7**, 649 (1954).
- [41] P. Pechukas and J. C. Light, J. Chem. Phys. **44**, 3897 (1966).
- [42] R. A. Marcus, J. Chem. Phys. **52**, 4803 (1970).
- [43] W. A. Cady, J. Chem. Phys. **60**, 3318 (1974).
- [44] J. S. Waugh, J. Magn. Reson. **50**, 30 (1982).
- [45] I. Schek, J. Jortner, and M. L. Sage, Chem. Phys. **59**, 11 (1981).
- [46] J. Ishikawa, F. Riehle, J. Helmcke, and C. J. Bordé, Phys. Rev. A **49**, 4794 (1994).
- [47] F. Impens, P. Bouyer, and C. J. Bordé, Appl. Phys. B **84**, 603 (2006).
- [48] A. Gauguet *et al.* Phys. Rev. A **78**, 043615 (2008).
- [49] K.J. Hughes, J.H.T. Burke, and C.A. Sackett, e-print arXiv:0902.0109 and to appear in Phys. Rev. Lett. (2009).
- [50] G. Whyte, P. Öhberg, and J. Courtial, Phys. Rev. A **69**, 053610 (2004).
- [51] D. R. Murray and P. Öhberg, JOSA B:Optical Physics **38**, 1227 (2005).
- [52] M. Weitz, B. C. Young, and S. Chu, Phys. Rev. A **50**, 2438 (1994).
- [53] C. Pare and P. Belanger, Optical and Quantum Electronics **24**, S1051 (1992).
- [54] L. P. Pitaevskii and A. Rosch, Phys. Rev. A **55**, R853 (1997).
- [55] F. Impens, e-print arXiv:0904.0150 and submitted to Phys. Rev. A (2009).

- [56] P. Cladé *et al.*, Eur. Phys. Lett. **71**, 730 (2005).
- [57] P. Bouyer and M.A. Kasevich, Phys. Rev. A **56**, R1083 (1997); S. Gupta *et al.*, Phys. Rev. Lett. **89**, 140401 (2002); Y.-J. Wang *et al.*, Phys. Rev. Lett. **94**, 090405 (2005); Y. LeCoq *et al.*, Appl. Phys. B: Laser and Optics **84**, 627 (2006).
- [58] J. Chen, Z. Zhang, Y. Liu, and Q. Lin, Opt. Expr. **16**, 10918 (2008).
- [59] Ch. J. Bordé, Eur. Phys. Jour. Spec. Top. **48**, 315 (2008); Ch. J. Bordé, in *Proc. of the Enrico Fermi International School of Physics*, Course CLXVIII (IOS Press, 2007)